

Weibull distribution based constitutive model for nonlinear analysis of RC beams

A. Ramachandra Murthy^{*1} and D. Shanmuga Priya^{2a}

¹CSIR-Structural Engineering Research Centre, Taramani, Chennai, 600113, India

²Dhanalakshmi College of Engineering, Chennai, Tamilnadu, 601301, India

(Received April 18, 2016, Revised October 13, 2016, Accepted October 31, 2016)

Abstract. Reinforced concrete is a complex material to be modeled in finite element domain. A proper material model is necessary to represent the nonlinear behaviour accurately. Though the nonlinear analysis of RC structures evolved long back, still an accurate and reliable model to predict the realistic behaviour of components are limited. It is observed from literature that there are three well-known models to represent the nonlinear behaviour of concrete. These models include Chu model (1985), Hsu model (1994) and Saenz model (1964). A new stress-strain model based on Weibull distribution has been proposed in the present study. The objective of the present study is to analyze a reinforced concrete beam under flexural loading by employing all the models. Nonlinear behaviour of concrete is considered in terms of stress vs. strain, damage parameter, tension stiffening behaviour etc. The ductility of the RC beams is computed by using deflection based and energy based concepts. Both deflection ductility and energy based ductility is compared and energy based concept is found to be in good correlation with the experiments conducted. The behavior of RC beam predicted using ABAQUS has been compared with the corresponding experimental observations. Comparison between numerical and experimental results confirms that these four constitutive models are reliable in predicting the behaviour of RC structures and any of the models can be employed for analysis.

Keywords: RC beam; Weibull distribution; ABAQUS; finite element analysis; ductility

1. Introduction

Reinforced concrete (RC) structures are generally designed to satisfy serviceability and safety criteria. To safeguard the serviceability requirement, it is mandatory to predict the crack pattern and deflection of the structures accurately under defined loads (Hyo *et al.* 2001). On the other hand, to assess the safety of structure against failure, an accurate prediction of the behaviour of RC structures/components is necessary. In particular, for comprehensive assessment of the strength, stiffness, and ductility of the RC structures, a nonlinear analysis is strongly required. Even though experiments can provide complete information regarding the behaviour of the members tested, it is very difficult to carry out experiments continuously and it is uneconomical and time-consuming. Therefore it is necessary to develop reliable analytical methods. Extensive studies by various researchers have led to the development of numerous constitutive models.

Hsu *et al.* (1994) developed a unified theory for reinforced concrete structures subjected to shear, torsion, bending and axial load. This theory is capable of predicting strength and load-deflection history of a member.

Alwathaf *et al.* (2011) investigated the behavior of reinforced concrete structures by proven stress-strain

models like Saenz model (1964) and Chu model (1985). Satisfactory results were obtained between developed FE model and experimental results.

Hu *et al.* (2010), Koksai *et al.* (2006) and Hamid *et al.* (2012) investigated the nonlinear behavior of reinforced concrete using Saenz's model (1964) to represent the stress-strain behavior of concrete. These models were tested against a series of experiments and good correlation was observed. Bathe *et al.* (1989) predicted the behaviour of RC structures/components with little modifications of Saenz's model. The response of a beam and two reactor vessels were predicted by ADINA software. Bahrami *et al.* (2014) performed a numerical study on concrete-filled steel composite stub columns with steel stiffeners using finite element software LUSAS. Saenz's model was used to represent the nonlinear behaviour of concrete in compression. The load-axial shortening curves obtained were found close to tested specimens.

Wahalathantri *et al.* (2011), Sankar *et al.* (2014) and Mattar *et al.* (2016) employed a material model of Hsu (1994) to simulate the non-linear behavior of reinforced concrete elements. By comparing the predicted behaviour of load-displacement, load-strain and the cracking pattern with the corresponding experimental observations, it confirms the applicability of the model. Ahmed *et al.* (2012) investigated the reliability of Carreira and Chu (1985) model in assessing the nonlinear behavior of complex structures like full scale reinforced concrete floor. A one-story joist floor with wide shallow beams supported on columns was studied. The performance of the model is found to be satisfactory.

*Corresponding author, Ph.D.

E-mail: murthyarc@serc.res.in, murthycsdg@gmail.com

^aAssistant Professor

Dawari *et al.* (2014) studied the nonlinear behavior of RC beams under flexural loading using numerical method in order to avoid destructive testing and reduce cost of materials and manpower. In this paper, compressive uniaxial stress-strain relationship defined by Hognestad is implemented. The results are in close agreement with available literature. Francesco *et al.* (2016) evaluated the structural behavior of RC beams externally strengthened with Steel Reinforced Grout and Steel Reinforced Polymer systems through nonlinear finite element analysis. Compressive behavior of concrete is represented by stress-strain model proposed by Hognestad. The numerical results in terms of load-displacement, failure mode were found satisfactory compared to experimental work.

Hasan *et al.* (2015) had performed nonlinear finite element analysis on RC haunched beams to predict its ultimate shear capacity. The numerical models were verified by experimental studies and the results were found to be in good agreement. Rajagopal *et al.* (2014) studied the nonlinear seismic behavior of RC exterior beam-column joint under reversal loading with different anchorage and joint core details. The analytical and experimental results were compared and found to be satisfactory.

From the limited literature, it can be observed that the relative performance of all the listed models is not available. The present study is aimed at to compare the response behaviour of the above models with the corresponding experimental observations. Further, a new constitutive model based on Weibull distribution is proposed to represent the nonlinear behaviour of concrete.

2. Material model

A brief description of the four constitutive stress-strain models is presented below.

2.1 Saenz model (1964)

The stress-strain relationship proposed by Saenz (Hsuam *et al.* 1989) is widely accepted as the uniaxial stress-strain curve for concrete and it is shown in Eq. (1)

$$\sigma_c = \frac{E_c \varepsilon_c}{1 + (R + R_E - 2) \left(\frac{\varepsilon_c}{\varepsilon_o}\right) - (2R - 1) \left(\frac{\varepsilon_c}{\varepsilon_o}\right)^2 + R \left(\frac{\varepsilon_c}{\varepsilon_o}\right)^3} \quad (1)$$

Where

$$R = \frac{R_E (R_\sigma - 1)}{(R_E - 1)^2} - \frac{1}{R_E}, \quad (2)$$

$$R_E = \frac{E_c}{E_o}, \quad (3)$$

$$E_o = f'_c / \varepsilon_o \quad (4)$$

Here R_σ and R_c can be taken as 4 (Hsuam *et al.* 1989) and ε_o and f'_c are the maximum strain and corresponding stress on the uniaxial stress-strain curve. Based on the above equations a typical stress-strain relationship for M30 concrete is deduced

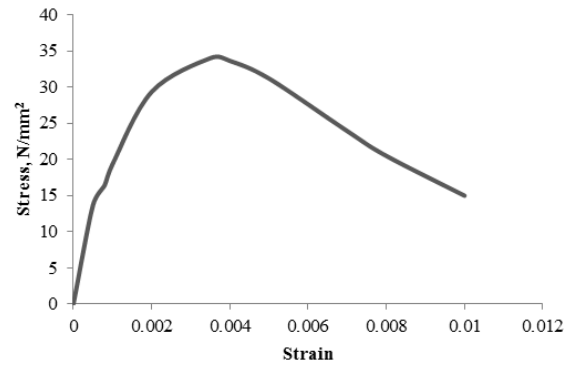


Fig. 1 Stress-strain model by Saenz (1964)

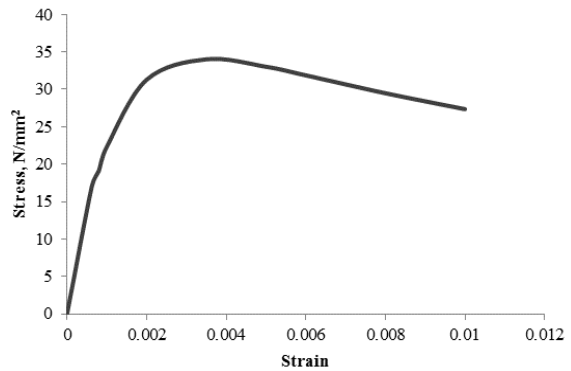


Fig. 2 Stress-strain model by Carreira and Chu (1985)

and shown in Fig. 1.

2.2 Carreira and Chu model (1985)

In an effort to construct a simple mathematical model that can represent the stress-strain behaviour of concrete with different compressive strength, the model developed by Carreira and Chu (Carreira *et al.* 1985) is found to yield the actual stress-strain response. Eq. (5) illustrates the general equation for the stress-strain behavior proposed by Carreira and Chu (1985).

$$f_c = f'_c \frac{\beta(\varepsilon/\varepsilon_o)}{[\beta - 1(\varepsilon/\varepsilon_o)^\beta]} \quad (5)$$

$$\beta = \frac{1}{\left[1 - \left(\frac{f'_c}{E_o \varepsilon_o}\right)\right]} \quad (6)$$

Where β is material parameter; E_o is initial tangent modulus; ε_o is strain corresponding to maximum stress. Based on the above Eq. (5)-(6), a constitutive model predicted for typical M30 concrete is presented in Fig. 2.

2.3 Hsu model (1994)

The stress-strain curve for concrete under compression is derived using the experimentally verified method by Hsu (Tehmina *et al.* 2014). This model is valid up to a maximum compressive strength of 62 MPa. A linear stress-strain relationship which obeys Hooke's law is assumed up

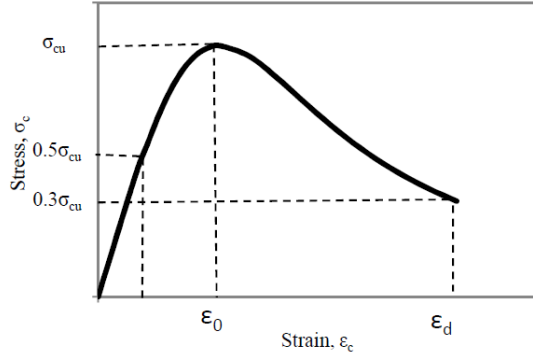


Fig. 3 Compressive behaviour of concrete (1994) (Wahalathantri *et al.* 2011)

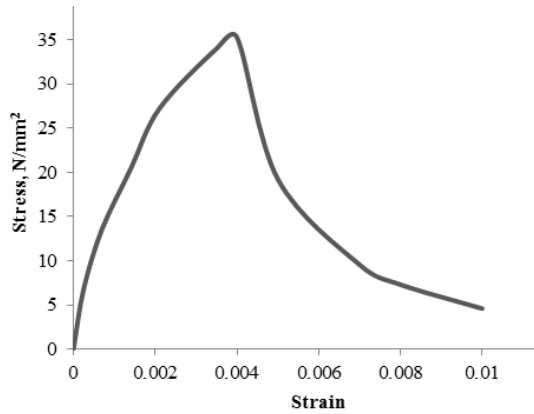


Fig. 5 Stress-strain model derived from Weibull distribution

to 50% of the ultimate compressive strength (σ_{cu}) in the ascending portion. The numerical model by Hsu (1994) is used to calculate the compressive stress values in the nonlinear region up to $0.3\sigma_{cu}$ and $n=1$. Governing equations are presented below.

$$\sigma_c = \left(\frac{n\beta(\varepsilon_c/\varepsilon_o)}{n\beta - 1 + (\varepsilon_c/\varepsilon_o)^{n\beta}} \right) \sigma_{cu} \quad (7)$$

$$\beta = \left(\frac{f'_c}{65.23} \right)^3 + 2.59 \quad (8)$$

$$\varepsilon_o = (1680 + 7.1f'_c) \times 10^{-6} \quad (9)$$

Where, the parameter β which depends on the shape of the stress-strain diagram which is derived from Eq. (8) and the strain at peak stress ε_o is given by Eq. (9). Fig. 3 shows the typical compressive stress-strain diagram for concrete according to Hsu model.

The material model derived for representing the compressive behaviour of typical M30 grade concrete is shown in Fig. 4.

2.4 Weibull distribution

Weibull distribution is continuous. It is usually applied in strength theory of brittle materials. It is adopted to represent the heterogeneity of concrete (Peiyinga *et al.* 2012). The probability dense function of Weibull

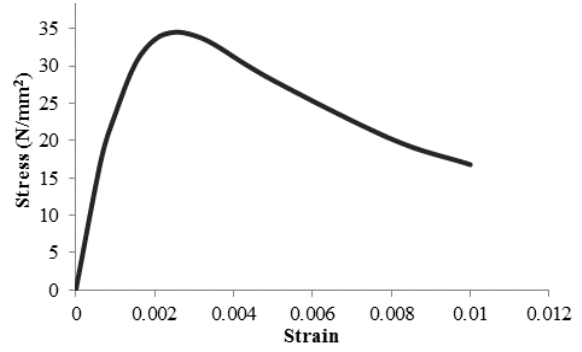


Fig. 4 Stress-strain model by Hsu (1994)

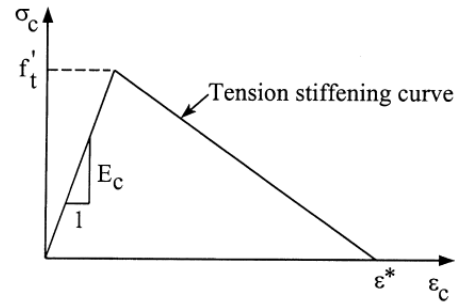


Fig. 6 Linear tension curve (Hu *et al.* 2010)

distribution is given by Eq. (10)

$$f(x) = \frac{\alpha}{\beta} \left(\frac{x}{\beta} \right)^{\alpha-1} \exp \left[- \left(\frac{x}{\beta} \right)^\alpha \right], x \geq 0 \quad (10)$$

Here x could be the elastic modulus, strength, Poisson's ratio and mass density, indicating that these properties conform to Weibull distribution (Peiyinga *et al.* 2012). β is average value of these mechanical properties and α is defined as the homogeneity index of concrete.

When the stresses evolve beyond the ultimate stress envelope, concrete exhibits some residual stress, i.e. damage is not hundred percent (Mao *et al.* 2006). The partial damage is described by a damage variable D indicated in Eq. (11) which follows two-parameter Weibull function as follows (Mazars 1986)

$$D = 1 - \exp \left[- \alpha \left(\frac{\varepsilon - \varepsilon_u}{\varepsilon_u} \right)^m \right] \quad (11)$$

Where ε_u is threshold strain, α and m are weibull parameters. The stress-strain relationship changes from $\sigma = \varepsilon E$ for undamaged concrete to $\sigma = E\varepsilon(1-D)$, from which

$$D = 1 - \frac{\sigma}{E\varepsilon} \quad (12)$$

Equating Eqs. (11) and (12)

$$\sigma = E\varepsilon \exp \left[- \alpha \left(\frac{\varepsilon - \varepsilon_u}{\varepsilon_u} \right)^m \right] \quad (13)$$

This equation is applicable for stress formulations after reaching ultimate stress. From this a typical stress-strain curve is formulated for M30 concrete as shown in Fig. 5.

All the four stress-strain models discussed above correspond to the compressive behaviour of concrete.

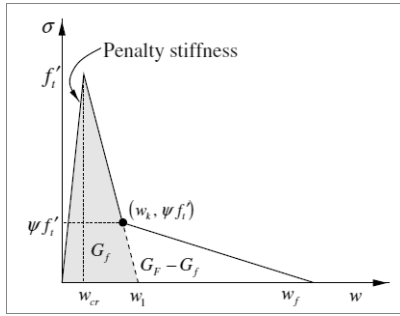


Fig. 7 Bilinear softening curve (Kyoungsoo 2008)

2.5 Tensile behaviour of concrete

Various tension stiffening models are available in the literature. Two models are adopted in the present study (Fig. 6 and Fig. 7). The descending portion accurately captures the primary and secondary cracking effect.

3. Nonlinear analysis of RC beam

3.1 Details of the beams

The dimensions of the beam are 100×200 mm in cross-section and 1500 mm in length. The beams are reinforced with 2-10 mm diameter bars at the tension and 2-8 mm diameter bars at the compression faces. Beams are provided with 6 mm diameter transverse reinforcement at 100 mm center-to-center as shown in Fig. 8.

Nonlinear analysis of the RC beam is carried out using a general purpose finite element software ABAQUS. The concrete beam was modeled with the brick elements to

achieve the uniform stress distribution. C3D8R (Cube Three Dimensional eight node Reduced integration) elements with 3 degrees of freedom at each node were used to model concrete part of beam. Reinforcing Steel bars were modeled as three dimensional truss elements (T3D2) having three translational degrees of freedom at each node. The beams were analyzed under four point loading with simply supported end conditions, over an effective span of 1200 mm. In order to simulate the experimental conditions as closely as possible, two steel loading plates were modeled at the location of two loading points as shown in Fig. 9. The loads were applied at a distance of 200 mm from either side of the mid-span as shown in Fig. 10. The analysis was carried out using displacement control. Concrete Damage plasticity model is incorporated to define the heterogeneous nature of concrete.

The interaction between the concrete beam and reinforcing steel was defined as embedded region constraint. To maintain the mesh uniformity the size length of the seed was taken as 20 mm for the whole model.

3.2 Details of material properties

The internal steel reinforcing bars are hot-rolled with yield strength of 415 MPa. The stress-strain curves derived by using the four models are employed as input of the concrete damage plasticity model. Tensile cracking and compressive crushing of concrete are two assumed main failure mechanisms in this model. Furthermore, the degradation of material for both tension and compression behavior have been considered in this model. A brief description of the concrete damage plasticity model is discussed here. The concrete damage model uses three independent strength surfaces, namely, an initial yield

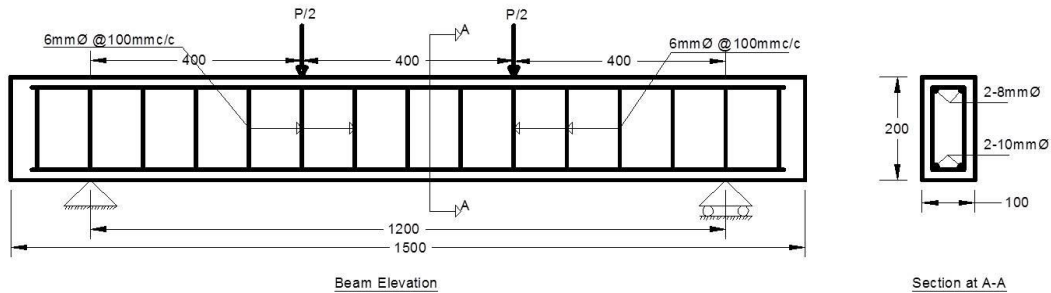


Fig. 8 Details of the beam

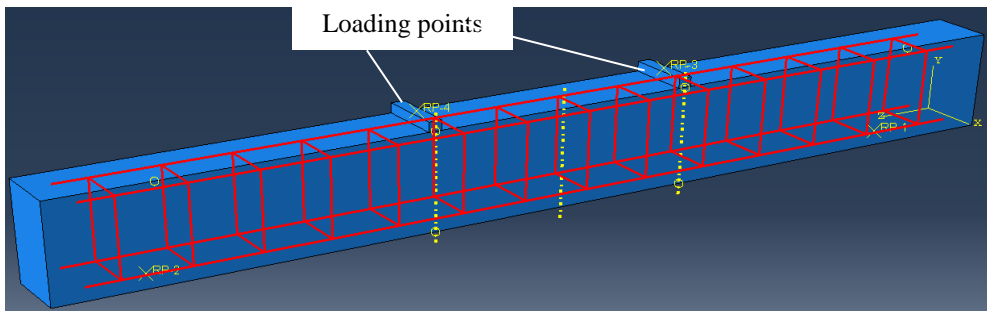


Fig. 9 Beam model assembled in ABAQUS

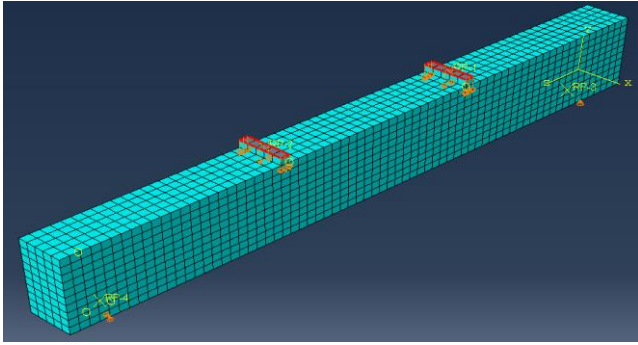
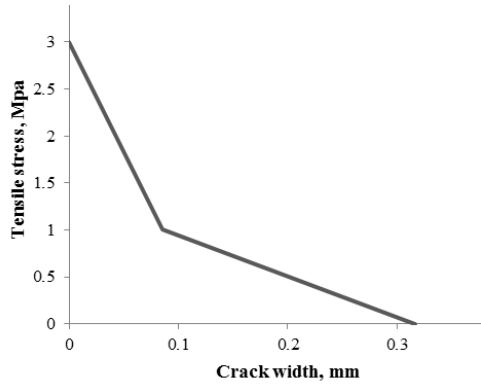


Fig. 10 Support and loading conditions

Fig. 11 Bilinear tension softening curve for concrete (Ramachandra Murthy *et al.* 2013)

surface, a maximum failure surface and a residual surface. The compressive meridians of the initial yield surface $\Delta\sigma_y^c$, the maximum failure surface $\Delta\sigma_m^c$ and the residual surface $\Delta\sigma_r^c$ are defined independently as (Ramachandra Murthy and Palani *et al.* 2013)

$$\Delta\sigma_y^c = a_{0y} + \frac{p}{a_{1y} + a_{2y}p} \quad (14)$$

$$\Delta\sigma_m^c = a_0 + \frac{p}{a_1 + a_2p} \quad (15)$$

$$\Delta\sigma_r^c = \frac{p}{a_{1f} + a_{2f}p} \quad (16)$$

With the specification of the three strength surfaces, the loading surfaces representing strain hardening after yield are defined as

$$\Delta\sigma_L = \eta\Delta\sigma_m + (1-\eta)\Delta\sigma_y \quad (17)$$

The post-failure surfaces, denoted by $\Delta\sigma_{pf}$, are defined in a similar way by interpolating between the maximum failure surface $\Delta\sigma_m$ and the residual surface $\Delta\sigma_r$

$$\Delta\sigma_{pf} = \eta\Delta\sigma_m + (1-\eta)\Delta\sigma_r \quad (18)$$

The variable η in Eqs. (17) and (18) is called the yield scale factor.

The ratio of plastic strain to inelastic strain is assumed

as 0.7. The damage parameter in compression is computed by using Eq. (19) (Yang *et al.* 2016). Plastic properties of reinforcing steel are given in Table 1 and Table 2 gives the details of the inelastic properties of concrete.

$$d_c = 1 - \frac{\sigma}{0.3\varepsilon E_o + 0.7\sigma} \quad (19)$$

The bilinear tension softening parameters are taken from Ramachandra Murthy *et al.* (2013). The bilinear tension softening parameters for normal strength concrete (NSC) were determined corresponding to size independent fracture energy. The tension diagram for NSC is given below in Fig. 11.

4. Experimental program

The reinforced concrete beams with the detail reinforcement is designed as under reinforced as per Indian Standard and cast at the laboratory following standard procedure. In order to study the pure flexural behavior, the beam is designed with required shear stirrups. For all concrete beams, longitudinal reinforcements of two of 10 mm diameters in tension, two of 8 mm diameter rebars in compression as hanger and shear reinforcements, 2-legged stirrups of 6 mm diameter at 100 mm c/c spacing were used. Sufficient margin of cover to the main reinforcement was ensured. Experiments were conducted to validate the numerical model. Control beams were tested under two point static loading to determine the failure load. The load was applied using a servo controlled hydraulic actuator (400

Table 1 Plastic properties of steel

Yield stress, N/mm ²	Plastic strain
332	0
352	0.0001
373	0.0003
394	0.001
435	0.002
435	0.003
440	0.005
435	0.01
400	0.03
370	0.06



Fig. 12 Experimental setup of the beam

Table 2 Concrete damage plasticity properties

	Compressive behaviour			Tensile behaviour		
	Yield stress, N/mm ²	Inelastic strain	Damage variable Dc	Yield stress, N/mm ²	Cracking strain	Damage variable dt
Hsu model	17.25949	0	0			
	23.54135	0.000137	0.046708			
	30.20835	0.000392	0.097439	3	0	
	33.53075	0.000771	0.159698	0	0.01	
	34.51155	0.001235	0.22789			
	34.08201	0.00175	0.29735	Yield stress	Displacement	0
	32.89826	0.002294	0.364705	3		0.988
	28.07237	0.003971	0.53775	1	0	
	20.20548	0.007259	0.747022	0	0.085	
	16.78049	0.009385	0.821303		0.317	
11.65942	0.014572	0.911267				
Chu model	17	0	0			
	19.13271	0.000101	0.041713			
	22.32414	0.000185	0.063691	3	0	
	31.27052	0.000858	0.183984	0	0.01	
	34	0.002258	0.353062			
	33.00483	0.003795	0.485765	Yield stress	Displacement	0
	31.85561	0.004837	0.55505	3	0	0.988
	29.46941	0.006924	0.658741	1	0.085	
	27.34132	0.009002	0.730087	0	0.317	
	20.58147	0.019248	0.884842			
Saenz model	13.6	0	0			
	16.43255	0.0002	0.090892	3		
	19.3381	0.000294	0.110995	0	0	
	29.33828	0.000929	0.206397		0.01	
	34.00194	0.002258	0.353044	Yield stress	Displacement	0
	33.62108	0.002772	0.403862	3		0.988
	31.17876	0.003862	0.504346	1	0	
	23.91074	0.006127	0.677963	0	0.085	
	20.47074	0.007253	0.744295		0.317	
	14.96516	0.009454	0.838449			
Weibull	6.8	0	0			
	13.6	0.000203398	0.109428			
	20.4	0.000655097	0.208756	3	0	
	27.2	0.001106797	0.25055	0	0.01	
	34	0.002258496	0.353064			
	35.24902	0.002712888	0.387375	Yield stress	Displacement	0
	19.21159	0.004298492	0.64767	3	0	0.988
	9.544326	0.006651491	0.851316	1	0.085	
	7.299442	0.007733462	0.896953	0	0.317	
	4.591978	0.009832325	0.946213			
Plasticity	Dilation angle	Eccentricity	fbo/fco	K	Viscosity parameter	
	36	0.1	1.16	0.667	0	

f_{b_0}/f_{c_0} is the ratio of initial equibiaxial compressive yield stress to initial uniaxial yield stress

kN capacity) under displacement control with a loading rate of 0.5 mm/min. Fig. 12 shows the experimental setup.

The beam is simply supported with an effective span of 1.2 m. The beam was adequately instrumented to record its behaviour under load. Electrical strain gauges were used at

extreme compression face of concrete at midspan and internal steel reinforcement to measure strain. The concrete strain at the mid-section over the depth of the beam was measured with linear variable displacement transducers (LVDT) with a gauge length of 60 mm. The tests were

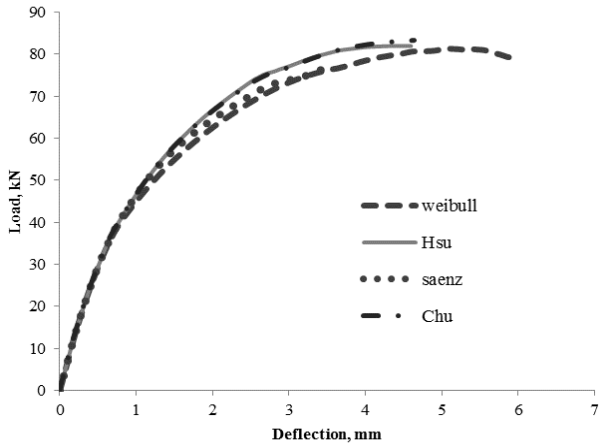


Fig. 13 Load-deflection behaviour of RC beam

carried out under displacement control conditions with relative ramp loading. All the vertical displacements measured using LVDTs are verified with actuator displacements. All the measurements were automatically recorded through data logger.

5. Results and discussion

5.1 Deformation behavior

The structural behaviour of the beams analyzed using the four stress-strain constitutive models for compressive behavior of concrete and linear tension softening behavior for steel is represented by their load-midspan deflection curves in Fig. 13. The observations show that load-deflection behaviour of the RC beam modeled using different material model is following a similar trend with small variations in load carrying capacity. Model derived from Weibull distribution has the capability to undergo large inelastic deformation when compared to others. The behaviour of the beam incorporated with Chu and Hsu material model is almost similar in both elastic and inelastic range, with 1% increase in ultimate load carrying capacity of Chu model. The advantage of this model is that it is simple and has the same general equation for use in both the ascending and the descending branch. In Hsu and Chu model, parameters are easy to find from the experimental data. Another observation from the analysis is that the RC beam incorporating bilinear tension softening model has the capability to predict larger deflections without failure in comparison to linear tension softening model (Fig. 14). The difference is very obvious in Chu and Saenz model. So, it is preferable to use bilinear tension softening behaviour of concrete for nonlinear analysis. A comparison of load carrying capacity and deflection for all the four models is presented in Table 3 which shows a good correlation of the newly proposed material model using Weibull distribution with the other three well-known models. Figs. 15, 16, 17 and 18 show the deformation/ deflection of the RC beam incorporating different material models using finite element analysis.

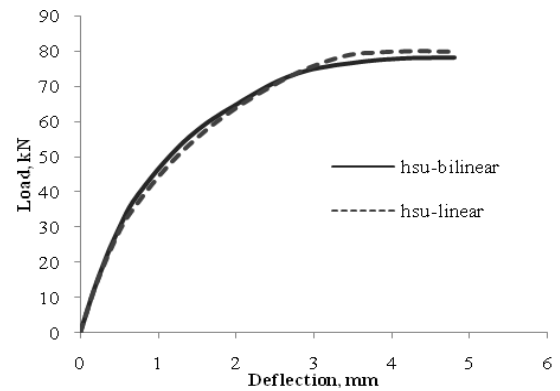


Fig. 14 (a) Comparison of linear and bilinear tension softening model - Hsu (1994)

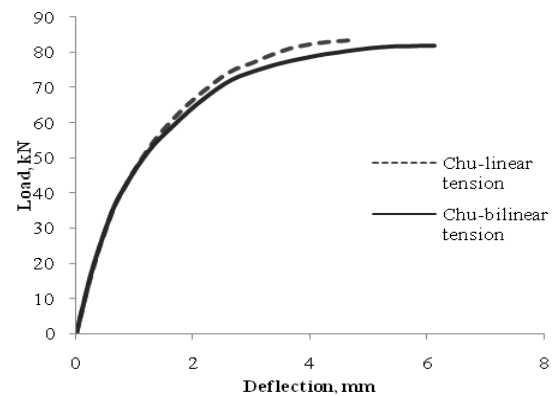


Fig. 14 (b) Comparison of linear and bilinear tension softening model - Chu (1985)

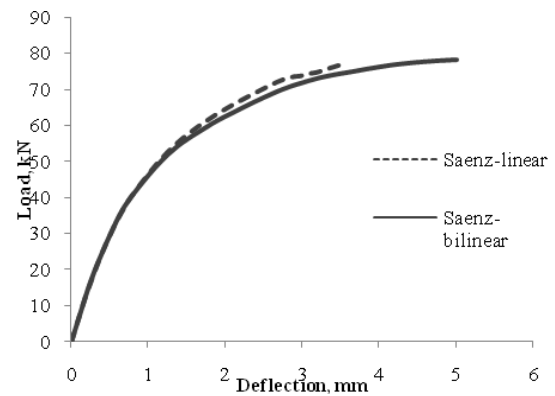


Fig. 14 (c) Comparison of linear and bilinear tension softening model - Saenz (1964)

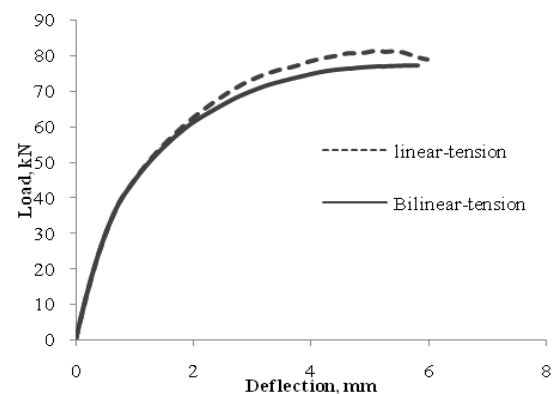


Fig. 14 (d) Comparison of linear and bilinear tension softening model - Weibull distribution

Table 3 Ultimate load and deflection

	Ultimate load (kN)	Deflection (mm)	Failure mode
Chu model	81.73	6.1	Tension steel
Saenz model	78.07	5.003	yielding,
Hsu model	78.24	4.80	concrete
Weibull	77.37	5.825	crushing

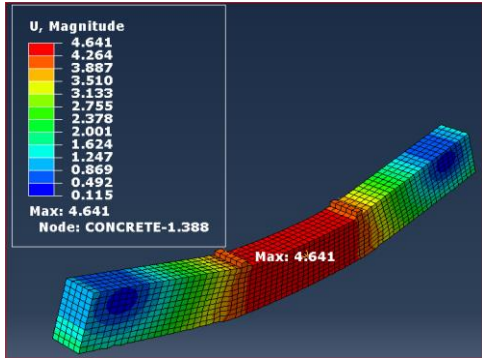


Fig. 15 (a) Deformation (Chu model 1985)-linear

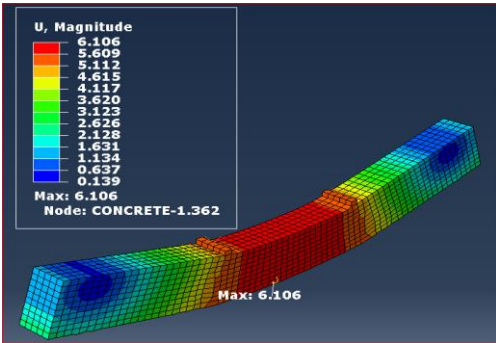


Fig. 15 (b) Deformation (Chu model 1985)-bilinear

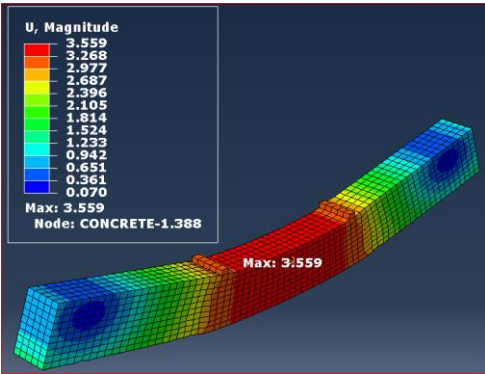


Fig. 16 (a) Deformation (Saenz model 1964)-linear

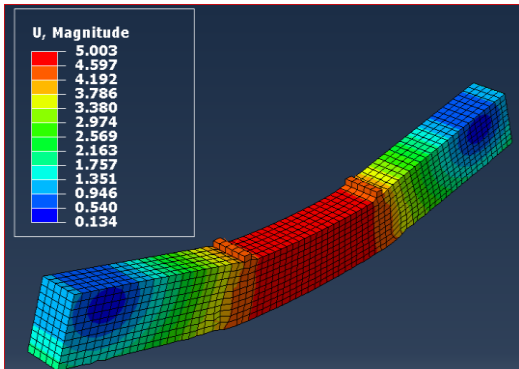


Fig. 16 (b) Deformation (Saenz model 1964)-bilinear

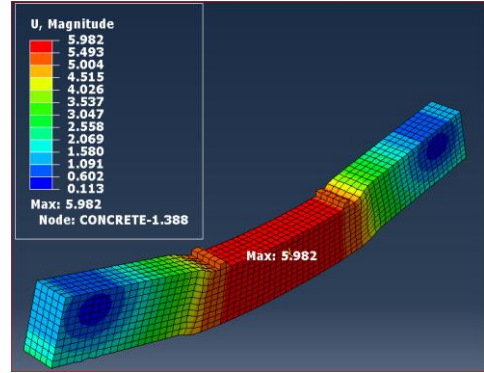


Fig. 17 (a) Deformation (Weibull distribution)-linear

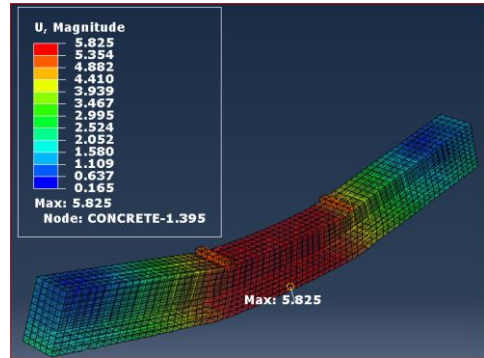


Fig. 17 (b) Deformation (Weibull distribution)-bilinear

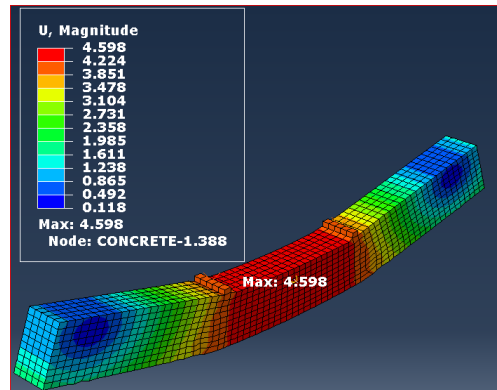


Fig. 18 (a) Deformation (Hsu model 1994)-linear

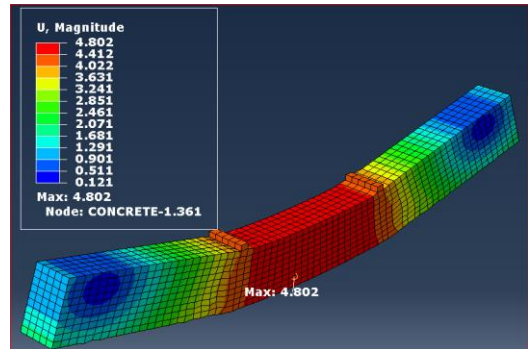


Fig. 18 (b) Deformation (Hsu model 1994)-bilinear

5.2 Comparison with experimental behavior

Fig. 19 shows the of load-deflection curves of numerical analysis and experiment under typical four point bending for RC beams. The stiffness of the beam analyzed is found

Table 4 Structural response of RC beams

	Chu model	Saenz model	Hsu model	Weibull	Experiment
Load at first crack (kN)	23.128 (27.75% of P_u)	23.128 (30% of P_u)	23.128 (28.2% of P_u)	23.128 (28.6% of P_u)	26 (31% of P_u)
Load at tension steel yielding (kN)	59.69 (71.6% of P_u)	54.63 (70% of P_u)	57.16 (70.2% of P_u)	59.66 (73.8% of P_u)	64.8 (77.8% of p_u)

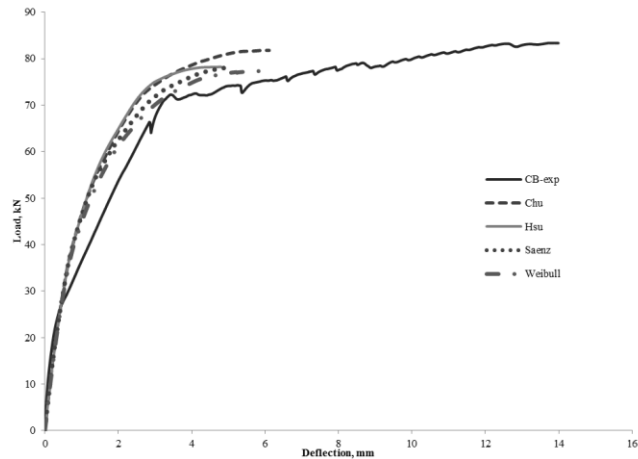


Fig. 19 Load-deflection curve of RC beams

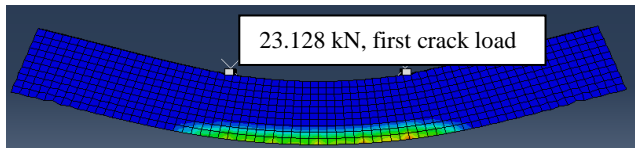


Fig. 20 (a) Load at first crack

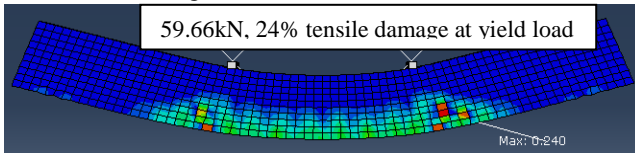


Fig. 20 (b) Tensile damage at yield load

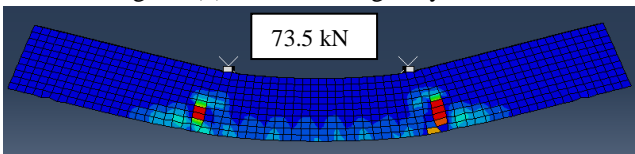


Fig. 20 (c) Load at 50% penetration of flexural crack

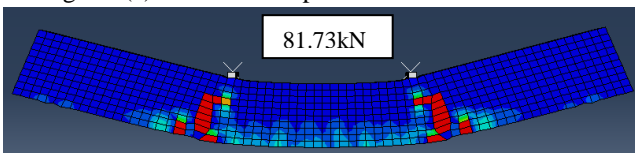


Fig. 20 (d) Crack pattern at ultimate capacity of beam

to be less than experimental beam stiffness till 28 kN i.e., 34.56% of the ultimate load. Beyond this load the flexural stiffness of the beam analyzed with all four material models is comparatively higher than the tested beam. All the four stress-strain models are found to simulate the RC beam behaviour in close approximation to tested beam up to ultimate load. The structural response of the beams in terms

Table 5 Ultimate load and failure modes

	Ultimate load (kN)	Variation in ultimate capacity (%)	Failure mode
Chu model	81.73	2.06	Tension steel yielding, concrete crushing
Saenz model	78.07	6.44	
Hsu model	78.24	6.24	
Weibull distribution	77.37	7.28	
Experiment	83.45		

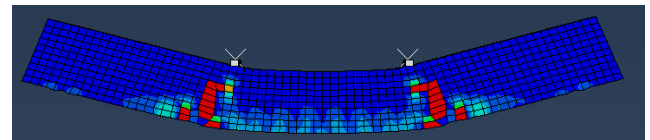


Fig. 21 Tensile damage-ABAQUS

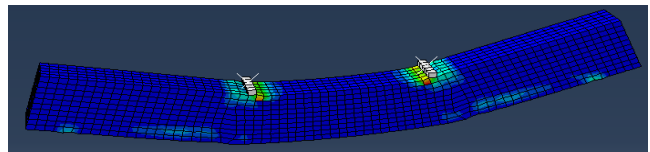


Fig. 22 Compression damage-ABAQUS

of load is shown in Table 4, which summarizes the load at first flexural crack and yielding of tension steel. For each model, the table also provides the percentage of these loads w.r.t to their ultimate load (P_u). Yield load corresponds to a significant decrease in the slope of the load-deflection plot. From the table, it is evident that RC beam analyzed using Weibull distribution based constitutive model gives the best performance among the other three.

Tensile damage and corresponding load is shown in Fig. 19 for RC beam modeled with Chu stress-strain curve as it gives the best results. In Fig. 20 (a) the red color at the bottom of the beam denotes the formation of first crack (b) tensile damage corresponding to yield load in the beam, (c) cracks below the two loading point penetrating up to half the depth of the beam, (d) cracks patterns at ultimate capacity of beam and the corresponding load.

5.3 Ultimate load and modes of failure

The ultimate load of the beams with different stress-strain models and their modes of failure in comparison to experimental beam are summarized in Table 5. The RC beam failed at an average ultimate load of 78.85 kN in flexure by yielding of tension steel followed by crushing of concrete in compression zone for all the four models.

Crack patterns or tensile damage in the beams as shown in Fig. 21 depicts that maximum damage occurs at the bottom of the beam under the loading point with penetration of the cracks up to 80% of the beam depth. Most cracks which have penetrated up to 50% of the depth of the beam are limited to the span in between the loading plates. Local crushing of concrete has taken place at the compression zone for a distance of 60 mm on either side of the loading point as shown in Fig. 22.

The failure mode in numerical analysis also confirms to

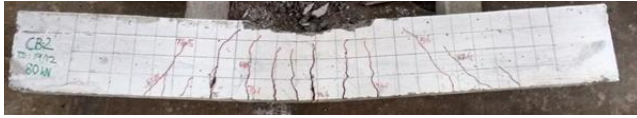


Fig. 23 (a) Failure mode-experiment- Beam1

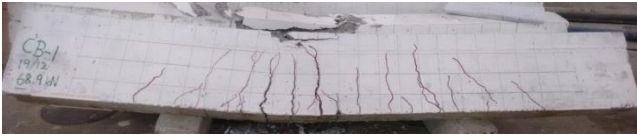


Fig. 23 (b) Failure mode-experiment- Beam2

the tested specimens as shown in Fig. 23. The presented results confirm that the numerical simulation of the RC beam using the four material models can predict the true behavior of RC elements.

5.4 Structural ductility

The load-deflection curves shown in Fig. 19 affect the overall structural ductility of the beam in terms of mid-span deflection and area under load-deflection plot. Deflection ductility and Energy ductility are evaluated at two different stages, yielding of tension steel and at ultimate failure given by Eqs. (20) and (21). Basically the ductility of the RC beams can be determined either using load-deflection curve or the moment curvature. They both are important as load deflection response of any structural member provides the inelastic deformation capability, whereas moment curvature provides the true rotational behavior of the section during failure. Energy based ductility is found to be more effective and realistic compared to deflection ductility as it incorporates deflection as well as energy absorbed during the ultimate collapse.

Deflection ductility

$$\mu_{\Delta} = \Delta_u / \Delta_y \quad (20)$$

Energy ductility

$$\mu_E = E_{total} / E_y \quad (21)$$

Where

Δ_u =midspan deflection at ultimate load

Δ_y =midspan deflection at yield load

E_{total} =area under load-deflection diagram at ultimate load

E_y =area under load-deflection diagram at yield load

The calculated ductility indices are shown in Table 6. A minor reduction of the ductility is observed for all the modeled beams in comparison to tested specimens. The ductility of Hsu and Chu model based on energy is found to be satisfactory when compared to the experiment with only 2.65% reduction. On the otherhand, the ductility of beam incorporating Weibull distribution is increased by 4% in comparison to tested specimen.

6. Conclusions

The numerical and experimental investigations were carried out to study the structural behavior of the RC beams

Table 6 Ductility indices

	Chu model	Saenz model	Hsu model	Weibull	Experiment
Deflection ductility	2.93	2.29	2.93	3.42	4.19
Energy ductility	3.68	3.144	3.67	3.93	3.77

by employing three well-known models to represent the nonlinear behaviour of concrete. These models include Chu model (1985), Hsu model (1994) and Saenz model (1964). A new stress-strain model based on Weibull distribution has been proposed in the present study. Nonlinear behaviour of concrete is considered in terms of uniaxial compressive behaviour, tension softening behaviour and damage parameters. The important observation made from the study is that all the models perform in a similar way and any model can be employed for analysis and design of RC structures/elements. Load-deflection behaviour of the RC beam modeled using different material model is following a similar trend with only small acceptable variations in load carrying capacity. The first crack load, yield load, ultimate load and failure pattern obtained from numerical analysis are in good correlation with experiment. Chu model is the best among the four which simulates close resemblance to the tested RC beams. The new material model derived using Weibull distribution for representing the uniaxial stress-strain behaviour of concrete in compression also gives equivalent results to the other three models and shows increase in ductility. The failure mode observed in all the beams is typical flexure failure with yielding of tension steel followed by local crushing of concrete in compression zone. The ductility results highlights that the energy based ductility of the beams are found to be more effective and realistic compared to deflection ductility as it incorporates deflection as well as energy absorbed during the ultimate collapse. The minor reduction of the deflection ductility is observed in all beams however, the energy based ductility is found to be satisfactory. Hence it can be concluded that for the estimation of reliable ductility, energy based concept is preferable and any of the models can be employed for analysis of reinforced concrete beam.

Acknowledgements

Authors acknowledge the technical discussions and support provided by Computational Structural Mechanics Group of CSIR-SERC.

References

- Ahmed Shuraim, B. (2012), "Numerical forensic model for the diagnosis of a full-scale RC floor", *Latin Am. J. Solid. Struct.*, **1**, 1-19.
- Albegmprli, H.M., Cevik, A., Gulsan, M.E. and Kurtoglu, A.E. (2015), "Reliability analysis of reinforced concrete haunched beams shear capacity based on stochastic nonlinear FE analysis", *Comput. Concrete*, **15**(2), 259-277.

- Alwathaf, A.H., Ali, A., Jaafar, M.S. and Algorafi, M.A. (2011), "Stress-strain modelling of reinforced concrete membrane structures", *Int. J. Phys. Sci.*, **6**(30), 6820-6828.
- Ayub, T., Shafiq, N. and Nuruddin, M.F. (2014), "Stress-strain response of high strength concrete and application of the existing models", *Res. J. App. Sci. Eng. Tech.*, **8**(10), 1174-1190.
- Bahrami, A., Badaruzzaman, W.H.W. and Osman, S.A. (2014), "Numerical study of concrete-filled steel composite stub columns with steel stiffeners", *Latin Am. J. Solid. Struct.*, **11**, 683-703.
- Bathe, K.J., Walczak, J., Welch, A. and Mistry, N. (1989), "Nonlinear analysis of concrete structures", *Comput. Struct.*, **32**(3), 563-590.
- Bencardino, F. and Condello, A. (2016), "3D FE Analysis of RC beams externally strengthened with SRG/SRP systems", *Fiber.*, **4**(19), 1-13.
- Carreira, D.J. and Chu, K.H. (1985), "Stress-strain relationship for plain concrete in compression", *J. Am. Concrete. I.*, **82**(6), 797-804.
- Dawari, V.B. and Vesmawala, G.R. (2014), "Application of nonlinear concrete model for finite element analysis of reinforced concrete beams", *Int. J. Sci. Eng. Res.*, **5**(9), 776-782.
- Hsu, T.T. (1994), "Unified theory of reinforced concrete-a summary", *Struct. Eng. Mech.*, **2**(1), 1-16.
- Hu, H.T., Lin, F.M., Liu, H.T., Huang, Y.F. and Pan, T.C. (2010), "Constitutive modeling of reinforced concrete and prestressed concrete structures strengthened by fiber-reinforced plastics", *Compos. Struct.*, **92**, 1640-1650.
- Hu, H.T. and Schnobrich, W.C. (1989), "Constitutive modeling of concrete by using non-associated plasticity", *J. Mater. Civil. Eng.*, ASCE, **1**(4), 199-216.
- Koksal, H.O. (2006), "A failure criterion for RC members under triaxial compression", *Struct. Eng. Mech.*, **24**(2), 137-154.
- Kwak, H.G. and Kim, S.P. (2001), "Nonlinear analysis of RC beam subject to cyclic loading", *J. Struct. Eng.*, ASCE, **127**(12), 1436-1444.
- Mattar, I.S.A.I. (2016), "Nonlinear FE model for RC beams shear-strengthened with FRP", *Mag. Concrete Res.*, **68**(1), 12-23.
- Murthy, A.R., Palani, G.S., Gopinath, S., Kumar, V.R. and Iyer, N.R. (2013), "An improved concrete damage model for impact analysis of concrete structural components by using finite element method", *CMC: Comput. Mater. Continua*, **37**(2), 77-96.
- Murthy, A.R., Karihaloo, B.L., Iyer, N.R. and Prasad, B.R. (2013), "Bilinear tension softening diagrams of concrete mixes corresponding to their size-independent specific fracture energy", *Constr. Build. Mater.*, **47**, 1160-1166.
- Park, K., Paulino, G.H. and Roesler, J.R. (2008), "Determination of the kink point in the bilinear softening model for concrete", *Eng. Fract. Mech.*, **75**, 3806-3818.
- Peiying, G., Chang, D. and Lei, T. (2012), "Determination of local damage probability in concrete structure", *Procedia Eng.*, **28**, 489-493.
- Rajagopal, S., Prabavathy, S. and Kang, T.H.K. (2014), "Seismic behavior evaluation of exterior beam-column joints with headed or hooked bars using nonlinear finite element analysis", *Earthq. Struct.*, **7**(5), 861-875.
- Sankar Jegadesh, J.S. and Jayalekshmi, S. (2014), "Numerical analysis of RC shear critical beams", *Int. J. Struct. Civil Eng. Res.*, **3**(1), 69-75.
- Sinaei, H., Shariati, M., Abna, A.H., Aghaei, M. and Shariati, A. (2012), "Evaluation of reinforced concrete beam behaviour using finite element analysis by ABAQUS", *Scientif. Res. Essay*, **7**(21), 2002-2009.
- Wahalathantri, B.L., Thambiratnam, D.P., Chan, T.H.T. and Fawzia, S. (2011), "A material model for flexural crack simulation in reinforced concrete elements using ABAQUS", *Proc. of International Conference on Engineering*, Queensland University of Technology, Brisbane.
- Yang, K., Li, W. et al., (2016), "Constitution and application of RPC constitutive model", *J. Struct. Eng.*, **2**(6), 565-572.
- Yu, M.H. (2006), *Generalized Plasticity*, Springer Science & Business Media.

CC